

Heat-treated polyacrylonitrile-based catalysts for oxygen electroreduction

S. GUPTA, D. TRYK, I. BAE, W. ALDRED, E. YEAGER

Case Center for Electrochemical Sciences and The Chemistry Department, Case Western Reserve University, Cleveland, OH 44106-2699, USA

Received 29 March 1988; revised 27 June 1988

Polyacrylonitrile (PAN), mixed with Co(II) or Fe(II) salts and high-area carbon and then heat treated, has been found to yield very promising catalysts for O₂ reduction in concentrated alkaline and acid solutions. The catalytic activities are comparable to those for the heat-treated corresponding transition metal macrocycles and polypyrrole black-based catalysts. The addition of the transition metal to the nitrogen-containing polymer, either before or after the heat treatment with carbon, is an important factor for good activity. The nitrile nitrogen of the PAN is probably retained and converted to pyridyl nitrogen during the heat treatment, and this nitrogen is believed to provide binding sites for the transition metal ions, which then act as catalytic sites for oxygen reduction to peroxide and its decomposition.

1. Introduction

Various research groups [1-9] have reported that the heat treatment (up to ~1000°C) of transition metal macrocycles together with high-area carbons significantly improves their stability as electrocatalysts for O₂ reduction in alkaline and acid electrolytes without substantially degrading and, in some instances, enhancing their overall catalytic activity. Furthermore, it has been found that the transition metal need not be incorporated chemically in the macrocycle before the heat treatment in order to achieve a highly catalytic active material. Either iron or cobalt salts such as the acetates can be added before the heat treatment of the metal-free macrocycle such as the tetramethoxyphenyl porphyrin (H₂TMPP) and yield activity in alkaline and acid electrolytes comparable to that of the heat-treated corresponding metal-containing macrocycles [10-12].

The source of the catalytic activity in these heat-treated compounds is not completely understood, but the interaction between the transition metal and the nitrogen originally part of the macrocycle pyrrole ring is an important factor. Transition metal porphyrins contain four pyrrole nitrogens coordinated to the metal ion, but it is not well established to what extent this Me---N₄ structure remains intact after the heat treatment at 800°C and higher.

Recently McBreen *et al.* [13] have carried out EXAFS investigations on pyrolyzed iron and cobalt phthalocyanines and tetramethoxyphenyl porphyrins. According to these authors, the analysis of the data provides evidence that a significant amount of the cobalt retained in the heat-treated catalyst is still coordinated to four nitrogens of the porphyrin structure.

Based on various electrochemical and non-electro-

chemical studies of the heat-treated macrocycles and related complexes [14-16], our group has proposed a model to explain the catalytic activity of the heat-treated transition metal macrocycles. The model proposed is that of a modified carbon surface on which transition metal ions are adsorbed, principally through interactions with the residual nitrogen derived from the heat-treated macrocycles (Fig. 1). This model suggests the use of other electronically conducting surfaces with nitrogen groups capable of binding transition metal species as catalysts. Such catalysts have recently been prepared at Case by mixing pyrrole black polymer with transition metal salts (Fe or Co) and then heat treating them. The catalytic activities for O₂ reduction of these materials have been found to be comparable to those of the heat-treated corresponding transition metal macrocycles [14].

In order to see if other nitrogen-containing polymers can also be used in the preparation of active catalysts for O₂ electroreduction, experiments have been conducted with polyacrylonitrile (PAN). It is known that PAN can be made electronically conductive by various heat treatment conditions [17] and particularly in vacuum at temperatures between 390 and 435°C [18]. IR spectra show that the very large increase in conductivity is correlated with the formation of conjugated C=C and C=N bonds [18]. In the present study the catalysts were prepared by heat treating PAN mixed with transition metal salts and high-area carbon at various temperatures in an inert atmosphere (argon). The reduction of O₂ catalyzed by such materials has been studied in alkaline and acid electrolytes using porous gas-fed electrodes and the thin porous coating (TPC) rotating ring-disk electrode technique.

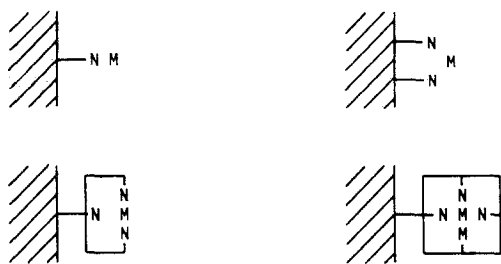


Fig. 1. Models for transition metal binding on heat-treated macrocycles; N = nitrogen; M = transition metal.

2. Experimental details

Polyacrylonitrile (Aldrich Chemical Company, molecular weight $\sim 150\,000$) was used without further purification. The high-area carbons used in the preparation of the catalysts were Vulcan XC-72 (Cabot Corp., Billerica, MA; BET area = $216\text{ m}^2\text{ g}^{-1}$, $\sim 0.01\text{--}0.02\text{ wt\% Fe}$); Shawinigan acetylene black (Chevron Chemical Co., Olefins and Derivatives Div., Houston, Texas) that was steam activated and supplied by Electromedia Corp., Englewood, NJ (SASB; BET area = $190\text{ m}^2\text{ g}^{-1}$, $\sim 0.002\text{ wt\% Fe}$) and RB carbon (Calgon Corp., Pittsburgh, PA; BET area = $1200\text{ m}^2\text{ g}^{-1}$, $\sim 0.31\text{ wt\% Fe}$), originally containing 23% ash and de-ashed to 2% by the Electromedia Corp. The catalysts were prepared by dissolving specified amounts of PAN together with either Co(II) or Fe(II) acetate in 100 ml of warm dimethylformamide (DMF), next mixing in a specified amount of carbon black and then removing the DMF by evaporation under 1 atm of N_2 . The solid samples were then heat-treated in a horizontal tube furnace at specified temperatures under continuous flow of purified argon (Matheson, HP grade) and allowed to cool while still under flowing argon.

Porous gas-fed electrodes (Fig. 2) were fabricated as reported earlier [14]. The fabrication procedure involves the use of a Teflon dispersion (DuPont T30B, containing Triton X-100 as a dispersing agent). The Teflon sintering temperature used in this work was $280\text{--}310^\circ\text{C}$. A nickel foil counter electrode and Hg/HgO, OH^- reference electrode were used in alkaline electrolytes; a platinum foil counter and a Hg/Hg₂HPO₄ reference electrode were used in acid electrolytes. For the latter, the potential was converted to the reversible hydrogen electrode (RHE) scale by adding 0.540 V [19]. The polarization curves were recorded under steady state conditions.

The O_2 reduction measurements for the porous gas-fed electrodes were performed galvanostatically in 4 M NaOH at 60°C and 85% H_3PO_4 at 100°C with a research potentiostat (Stonehart Associates, Madison, CT, Model BC-1200). This potentiostat includes *IR* drop compensation plus correction circuits. The *IR* drop correction adjustment is done while monitoring the potential on an oscilloscope as the current is repetitively interrupted for 0.1 ms every 1.1 ms. Correction is made only for the *IR* drop external to the porous active catalyst layer, however.

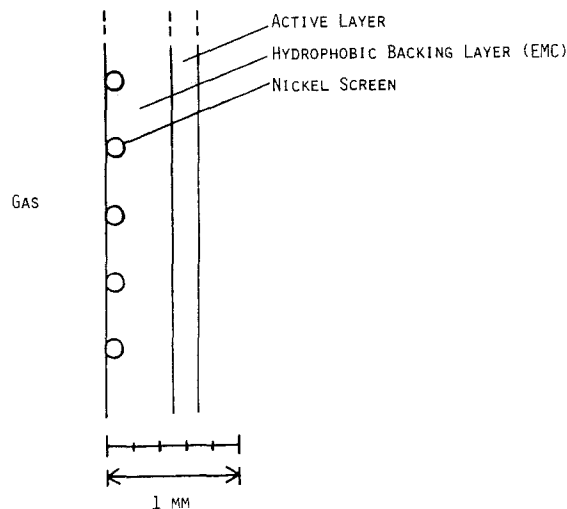


Fig. 2. Structure of the porous gas-fed electrode used for catalyst evaluation in alkaline electrolytes.

A thin porous Teflon-bonded layer ($\sim 5\text{ mg cm}^{-2}$, corresponding to a thickness of $\sim 50\ \mu\text{m}$) of the heat-treated material was applied on an ordinary pyrolytic graphite (OPG) disk (area: 0.196 cm^2), which was part of a rotating ring-disk electrode assembly [6]. The Teflon suspension used was Du Pont T-30B, with the Teflon $\sim 10\%$ w/w in the final active coating. Oxygen from the solution phase diffuses through the gas-filled channels within this layer to reach the wetted catalyst/carbon agglomerates. The Pt ring, with a collection efficiency (N) of 0.37, was used to monitor peroxide. It was activated prior to the measurements by holding its potential at $-0.9\text{ V vs Hg/HgO, OH}^-$ for 60 s in order to reduce the oxide layer and was maintained at a potential of $+0.1\text{ V vs Hg/HgO, OH}^-$ in the alkaline electrolyte. In the acid electrolyte, the ring was activated by holding its potential at $+0.1\text{ V vs RHE}$ for 60 s and was maintained at a potential of $+1.4\text{ V vs RHE}$. The electrolytes, 0.1 M NaOH (Baker, low in carbonate) and 0.05 M H_2SO_4 (Ultrex) were saturated with O_2 at 1 atm. Gold foil was used as the counter electrode, and a saturated calomel electrode (SCE) was used as the reference. The potentials were converted so as to refer to the Hg/HgO, OH^- reference in the alkaline electrolyte and to the reversible hydrogen electrode (RHE) in the acid electrolyte. The steady state ring and disk currents were recorded at progressively more negative disk potentials.

3. Results and discussion

3.1. Studies in alkaline solutions

Figure 3 gives the performance of gas-fed electrodes made from Co(II)- and Fe(II)-based PAN catalysts prepared at various heat-treatment temperatures (HTT). The current density at $-0.1\text{ V vs Hg/HgO, OH}^-$ was used as a relative measure of the performance, which is related to the catalytic activity. The optimum HTT was found to be between 700 and 900°C . It may be noted that the pyrrole black polymer-based catalysts containing these transition

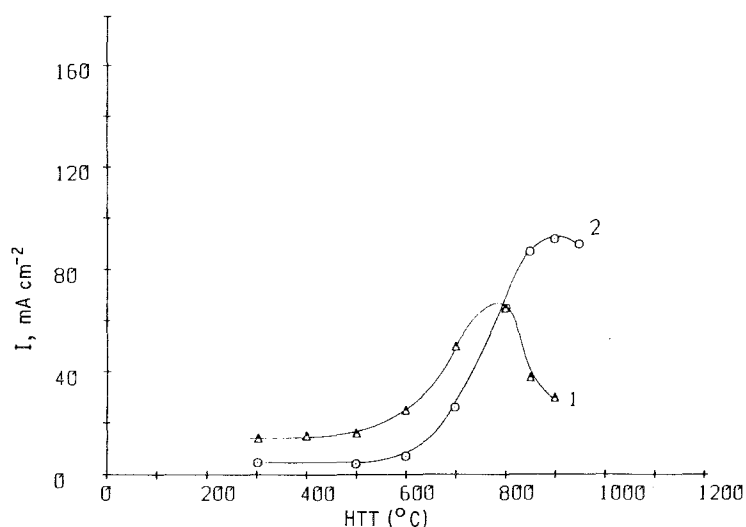


Fig. 3. Effect of heat-treatment temperatures on the apparent activity of Co- and Fe-based PAN catalysts. Apparent current density at -0.1 V vs Hg/HgO, OH^- for O_2 reduction using O_2 -fed electrodes in 4 M NaOH at 60°C vs heat-treatment temperature. Curve 1, 10% PAN + 0.59% Co (added as the acetate) + XC-72 carbon. Curve 2, 40% PAN + 1.60% Fe (added as the acetate) + XC-72 carbon. Electrodes were heat treated at various temperatures in flowing Ar for 2 h.

metals, with or without a carbon support, also showed maximum apparent activity for materials prepared at an HTT of $700\text{--}900^\circ\text{C}$ [14]. It should also be noted that if the currents are normalized, either for the number of moles of transition metal species or weight of PAN used in preparing the catalysts, the Co-based materials are seen to be more active.

The overall activity of the Co/PAN and Fe/PAN catalysts (optimum loading) is comparable with that of the heat-treated corresponding transition metal macrocycles and pyrrole black polymer-based catalysts containing the same transition metal ions (Figs 4 and 5). However, differences exist in the apparent activities, particularly for the Fe-based catalysts (i.e. FeTMPP < Fe/PAN < Fe/PB) as indicated by the polarization at lower current densities (e.g. $1\text{--}50\text{ mA cm}^{-2}$). At higher current densities the apparent activity with PAN- and polypyrrole black (PB)-based catalysts is lower than that of the macrocycle catalyst containing the same transition metal. This may be due to the fact that the electrode structures for PAN- and PB-based catalysts are not yet optimized.

Curves 1–3 in Fig. 6 indicate the polarization for heat-treated (800°C) Co/XC-72, PAN/XC-72 and Co/PAN/XC-72 catalysts, respectively. As seen earlier with heat-treated transition metal macrocycles [11, 12] and pyrrole black polymer-based catalysts [14], the transition metal or the nitrogen-containing polymer alone on carbon does not produce a good catalyst. The presence of both the transition metal and the nitrogen-containing polymer before (or after) the heat treatment with carbon is an important factor for high catalytic activity. It is interesting to note that substantial activity can be achieved by heat treating the PAN/carbon mixture without the transition metal but adding it in the form of $\text{Co}(\text{OH})_2$ or Co_3O_4 to the gas-fed electrode active layer and then activating the electrode in the electrolyte by driving the potential to very negative values. This activation process is not yet completely understood but may involve the insertion of cobalt ions into nitrogen-containing coordination sites. Cobalt in the +2 oxidation state is slightly soluble in the electrolyte (~ 60 ppm [20]) as the dicobaltite anion HCoO_2^- [21] or one of its hydrated

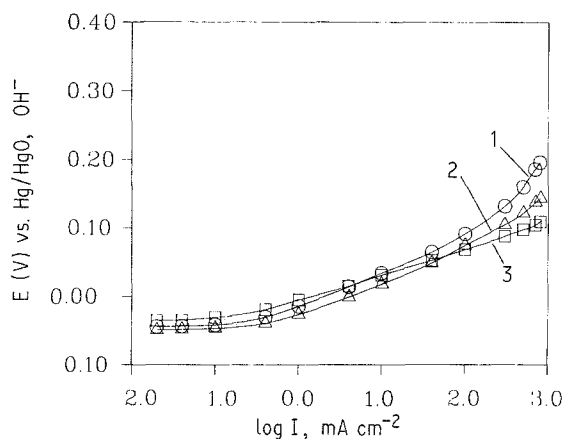


Fig. 4. Comparison of the overall activity of the Co/PAN catalyst with that of the heat-treated CoTMPP and pyrrole black polymer-based catalyst containing Co. Polarization curves for O_2 reduction with porous O_2 -fed (1 atm) electrodes in 4 M NaOH at 60°C ; catalyst/carbon 15.0 mg cm^{-2} and Teflon 6.4 mg cm^{-2} . Curve 1, PB + 2.5% Co (added as the acetate), 850°C HT. Curve 2, 40% PAN on XC-72 + 1.18% Co (added as the acetate), 800°C HT. Curve 3, 4.7% CoTMPP on XC-72, 450°C HT.

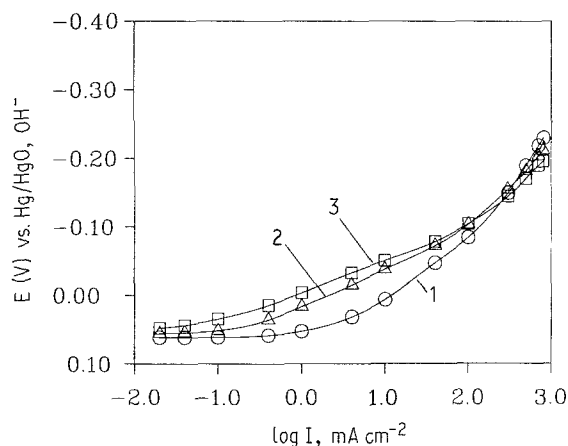


Fig. 5. Comparison of the overall activity of the Fe/PAN catalyst with that of the heat-treated $(\text{FeTMPP})_2\text{O}$ and pyrrole black polymer-based catalyst containing Fe. Polarization curves for O_2 reduction with porous O_2 -fed (1 atm) electrodes in 4 M NaOH at 60°C ; other conditions the same as in Fig. 4. Curve 1, PB + 2.5% Fe (added as the acetate), 850°C HT. Curve 2, 40% PAN on XC-72 + 1.6% Fe (added as the acetate), 800°C HT. Curve 3, 4.8% $(\text{FeTMPP})_2\text{O}$ on XC-72, 800°C HT.

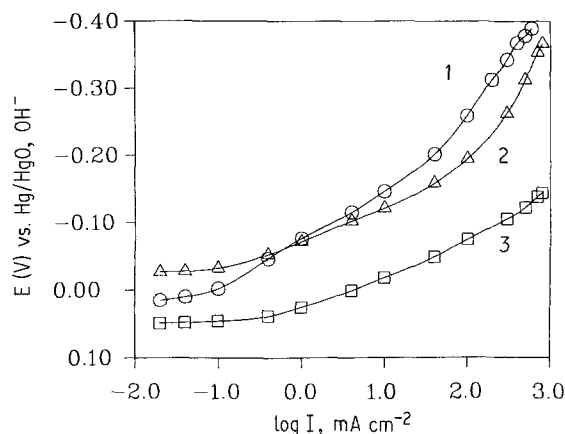


Fig. 6. Role of Co(II) ions in the heat-treated PAN-based catalysts. Polarization curves for O_2 reduction with porous O_2 -fed (1 atm) electrodes in 4M NaOH at 60°C; other conditions the same as in Fig. 4. Curve 1, XC-72 + 1.18% Co (added as the acetate), 800°C HT. Curve 2, 40% PAN + XC-72, 800°C HT. Curve 3, 40% PAN + 1.18% Co (added as the acetate) + XC-72, 800°C HT.

forms, e.g. $Co(OH)_3^-$. The negative potential may serve to favor the +2 state over the +3 state, which is otherwise more stable in the presence of O_2 [21].

Figure 7 indicates the polarization behavior of 40% PAN/XC-72 with 1.18% cobalt (added as the acetate) and heat-treated at 800°C in 4M NaOH at 60°C saturated with O_2 and air at 1 atm. The potential separation of the air and O_2 curves at low current densities is close to the 21 mV expected for a Nernstian response to the difference in O_2 partial pressures for a 2-electron process. This is consistent with peroxide decomposition as the rate-determining step with the O_2/HO_2^- couple essentially reversible. At high current densities, the deviation from the linear Tafel behavior for the O_2 curve may be due either to ohmic or mass transport polarization losses. These losses can be reduced by further optimization of the cathodes. The sharp upturn of the air curve is due principally to inhibited O_2 mass transport. Similar results were obtained for a catalyst made from 40% PAN/XC-72 with 1.60% Fe added as the acetate and heat-treated at 850°C. The deviation from linearity at higher

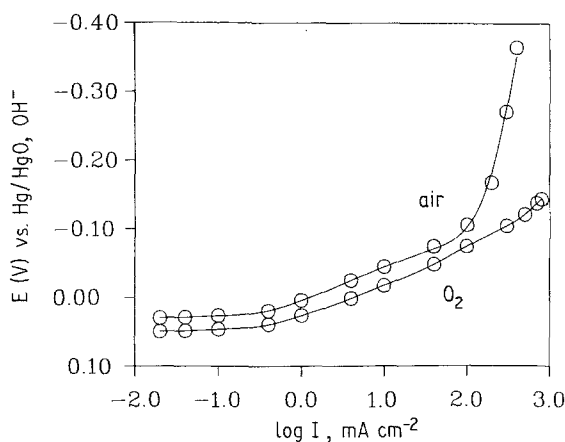


Fig. 7. Polarization behavior of a PAN-based catalyst with O_2 and air at 1 atm. Polarization curves for O_2 reduction with porous gas-fed (1 atm) electrodes in 4M NaOH at 60°C containing 40% PAN/XC-72 + 1.18% Co (added as the acetate), 800°C HT, for air and O_2 ; catalyst/carbon 15.0 mg cm^{-2} and Teflon 6.4 mg cm^{-2} .

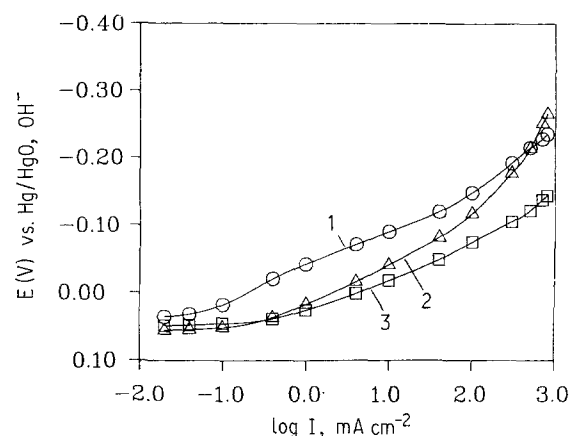


Fig. 8. O_2 reduction performance for the heat-treated PAN/XC-72 containing Co, Fe and Ru, respectively. Polarization curves for O_2 reduction with porous O_2 -fed (1 atm) electrodes in 4M NaOH at 60°C; other conditions the same as in Fig. 4. Curve 1, 40% PAN/XC-72 + 1.27% Ru (added as the acetylacetonate), 800°C HT. Curve 2, 40% PAN/XC-72 + 1.60% Fe (added as the acetate), 800°C HT. Curve 3, 40% PAN/XC-72 + 1.18% Co (added as the acetate), 800°C HT.

current densities on pure O_2 is more pronounced for the PAN/Fe catalyst (see Fig. 8) as compared to the PAN/Co catalyst.

Figure 8 shows the comparative behavior for O_2 reduction for 40% PAN/XC-72 containing Co, Fe and Ru, respectively, and heat-treated at 800°C. The apparent activity for the Co/PAN catalyst is better than those for the Fe/PAN or Ru/PAN catalysts at current densities above 1 mA cm^{-2} . The curves asymptotically approach a constant potential at lower current densities, where the system is under mixed potential control. The complementary anodic and cathodic reactions are probably carbon oxidation and oxygen reduction via the peroxide mechanism. If the carbon oxidation current-potential curve remains constant for the Co, Fe and Ru-PAN/carbon systems then the differences in potentials at low current densities can be explained by differences in peroxide decomposition activity. At higher current densities, the potential is controlled not only by the catalyst activity but also by the transport processes and ohmic losses within the active layer. When only activation control is involved, Tafel linearity is usually observed. For rate-determining peroxide decomposition, a -33 mV $decade^{-1}$ Tafel slope is expected at 60°C. The observed slopes for Co and Ru are relatively linear over more than two decades and close to -50 mV $decade^{-1}$ rather than -33 mV $decade^{-1}$. For Fe the curve has a more restricted Tafel linear region and the slope is higher. Anomalies in Tafel slopes can occur in porous gas-fed electrodes and may be responsible for Tafel slopes higher than that expected for the hydrogen peroxide decomposition step being rate controlling.

Efforts to improve the activity of the Co/PAN/C catalysts have included the use of (1) larger amounts of cobalt added as the acetate, e.g. 2.36% cobalt rather than 1.18% of the weight of carbon, (2) a larger fraction of PAN, e.g. 40% rather than 20% of the

Table 1. Effect of carbon substrates on the performance of O_2 -fed (1 atm) electrodes in 4 M NaOH at 60°C

Electrode material	Current density ($mA\ cm^{-2}$) at $-0.05\ V$ vs $Hg/HgO, OH^-$
SASB	0.20
XC-72	0.15
RB (de-ashed)	6.5
40% PAN/SASB + 1.18% Co	20.0
40% PAN/XC-72 + 1.18% Co	38.0
40% PAN/RB + 1.18% Co	60.0

total weight of carbon plus PAN before pyrolysis and (3) various types of carbons. The results show that the catalytic activity using 2.36% cobalt, however, was very similar to that obtained with the 1.18% cobalt. Use of 40% PAN instead of 20% made the material a little more active at all current densities except at very low current density. The increased activity after the heat treatment with the larger fraction of PAN may be due to an increased number of nitrogen sites that can bind the transition metal.

The performance at current densities below $\sim 100\ mA\ cm^{-2}$ of an electrode fabricated using material containing de-ashed RB carbon is better than that of ones using materials containing XC-72 or SASB carbons. These differences may be attributed either to the intrinsic properties of the carbon or to the transition metal impurities already present in the carbons, particularly with de-ashed RB carbon (see Table 1). The performance of the electrode made with de-ashed RB carbon however was worse than that of the electrodes made with XC-72 or SASB at higher current densities ($> 100\ mA\ cm^{-2}$). This may be due to specific characteristics of the RB carbon such as relatively large particle size (65–75% less than $44\ \mu m$) and high surface area ($\sim 1200\ m^2\ g^{-1}$), which may contribute to either high ohmic losses or to higher transport losses within the active catalyst layer. The Teflon content is also probably not optimum.

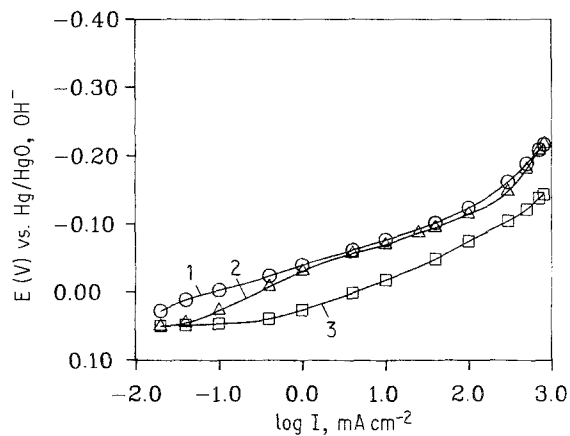


Fig. 9. O_2 reduction performance with heat-treated nitrogen-containing polymer-based catalysts with Co. Polarization curves with porous O_2 -fed (1 atm) electrodes in 4 M NaOH at 60°C. Curve 1, PVP/XC-72 + 1.18% Co, 800°C HT. Curve 2, PAA/XC-72 + 1.18% Co, 800°C HT. Curve 3, PAN/XC-72 + 1.18% Co, 800°C HT. Other conditions the same as in Fig. 7.

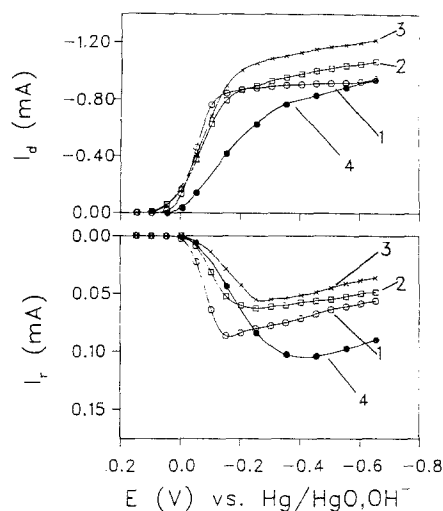


Fig. 10. Thin porous coating rotating ring-disk behavior for PAN-, PB- and macrocycle-based catalysts. Rotating ring-disk currents for O_2 reduction (1 atm) on thin porous coating (TPC) electrodes in 0.1 M NaOH at 25°C; disk area (geometric) = $0.196\ cm^2$; ring, Pt ($N = 0.37$), ring potential = $+0.1\ V$; 2500 rpm; Teflon = $\sim 10\%$. Curve 1, 5% CoTMPP/XC-72, 800°C HT. Curve 2, PB + 2.5% Co (added as the acetate), 800°C HT. Curve 3, 40% PAN/XC-72 + 1.18% Co (added as the acetate), 800°C HT. Curve 4, 40% PAN/XC-72, 800°C HT.

Experiments have also been conducted with other nitrogen-containing polymers such as polyvinyl pyridine (PVP) and polyacrylamide (PAA) mixed with cobalt acetate and XC-72 carbon in DMF and heat-treated at 800°C (Fig. 9, Curves 1 and 2, respectively). These polymers were treated in the same way as the PAN to render them conducting. These materials also show good activity for O_2 reduction but not as good as with Co/PAN/XC-72 (800°C HT) (Fig. 9, Curve 3). The ring-disk currents for O_2 reduction in 0.1 M NaOH on thin porous layers of 40% PAN/XC-72 with and without cobalt (1.18% added as the acetate), both heat-treated at 800°C show that the O_2 reduction activity is significantly increased by the presence of cobalt in PAN/XC-72 (Fig. 10, Curves 3 and 4). A similar trend is observed when these same types of materials are prepared without a carbon support. The O_2 reduction currents, however, are much smaller in the absence of the high-area carbon in the PAN materials. These heat-treated polymers exhibit semi-conducting properties. The higher performance with the high-area carbon support may be the combined result of the higher electronic conductivity of the electrode phase as well as the intrinsic catalytic activity of the carbon for the oxygen-to-peroxide reduction step.

An exact analytical treatment of the current-potential curves for the thin coated layer technique in relation to the kinetics is not yet available. Transport of O_2 within the active gas wicks is believed not to be rate controlling. The peroxide produced within the solution-filled pores, however, is slow to diffuse out of the layer, and the long residence time within the layer can result in increased peroxide decomposition (and possibly reduction) compared to the behavior with a non-porous disk electrode. Thus the standard analysis

of the rotating ring-disk data is not valid with the thin porous layer disk electrode. The effective number of electrons (n) transferred per O_2 molecule diffusing through the boundary layer can be calculated and is of interest in understanding various features of the catalysis. The $(\text{current})^{-1}$ vs $(\text{rotation rate})^{-1/2}$ plots [22] are linear, as expected for first-order kinetics for O_2 reduction. The apparent n values calculated from the slopes of these plots over the potential range -0.20 to -0.55 V are 4.0 for 40% PAN/XC-72 plus 1.18% Co and 3.1 for 40% PAN/XC-72 without Co. The predominant catalytic process is likely to be the decomposition of HO_2^- . PAN/XC-72 containing cobalt and heat-treated at 800°C has been found to be a good catalyst for the chemical decomposition of peroxide in 0.1 M NaOH solution with the catalyst dispersed in the electrolyte and using the gasometric technique to measure the volume of O_2 gas produced by the decomposition of HO_2^- as a function of time [23]. The fact that PAN/XC-72 heat-treated without the transition metal exhibited an n value greater than 2 probably indicates that there is some catalytic activity for peroxide decomposition and/or reduction.

Figure 10 also gives the comparative ring and disk currents for O_2 reduction using the thin porous electrode technique on PAN-, PB- and macrocycle-based catalysts containing cobalt and heat-treated at 800°C . The catalytic activity for O_2 reduction is similar for these materials, and the reduction follows the peroxide pathway. At low current densities no peroxide is detected on the ring, but this is probably due to the long time required for the peroxide to diffuse out of the porous electrode and the opportunity this affords for peroxide decomposition. The disk currents at higher cathodic potentials in the diffusion-controlled regime decrease in the following order: $\text{Co/PAN/XC-72} > \text{Co/PB} > \text{CoTMPP/XC-72}$, while the ring currents increase in the same order. None of the curves shows a well-defined diffusion-limiting current plateau. For Curve 1, the lack of a flat plateau in the limiting current region is due mostly to a slowly increasing n value (number of electrons per mole of O_2). The increase of the current in this region for the PB- and PAN-based catalysts (Curves 2 and 3) cannot be explained on the basis of such a change in n and appears to be an artifact of the porous coating technique due to roughness or hydrodynamic flow in the porous coating caused by the pressure gradient across the face of the disk. There is little hysteresis in this region for the data recorded with step-by-step increasing current and decreasing current.

3.2. Studies in acid solutions

The O_2 reduction polarization curves for the heat-treated PAN-based catalysts with XC-72 as the support in $85\% \text{ H}_3\text{PO}_4$ at 100°C in the form of porous gas-fed electrodes are given in Fig. 11. A polarization curve for heat-treated CoTMPP/XC-72 is also included for comparison. The apparent catalytic activity of the heat-treated Co/PAN/XC-72 is much

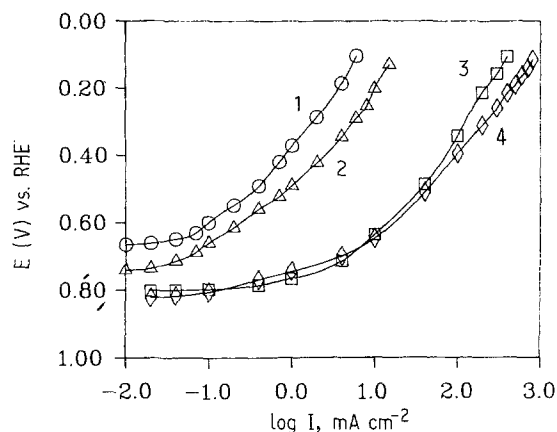


Fig. 11. Role of Co(II) ions in the heat-treated PAN-based catalysts. Polarization curves with porous O_2 -fed (1 atm) electrodes in $85\% \text{ H}_3\text{PO}_4$ at 100°C . All the electrodes contained 14.6 mg cm^{-2} catalyst/carbon and 6.2 mg cm^{-2} Teflon. Curve 1, XC-72, 800°C HT. Curve 2, 40% PAN/XC-72, 800°C HT. Curve 3, 40% PAN/XC-72 + 1.18% Co (added as the acetate), 800°C HT. Curve 4, 5% CoTMPP/XC-72, 800°C HT.

greater than that of the heat-treated XC-72 or PAN/XC-72 and similar to that of the heat-treated CoTMPP/XC-72. Figure 12 gives the polarization curves for these heat-treated materials supported on de-ashed RB carbon instead of XC-72. The overall performance of these catalysts is much better with de-ashed RB carbon as compared to XC-72 as the support. The better performance of the catalysts in $85\% \text{ H}_3\text{PO}_4$ at 100°C with de-ashed RB as the support may be due to its high surface area, mostly associated with the fine pore structure of the de-ashed RB carbon.

The heat-treated nitrogen-containing polymer-based cobalt catalysts as well as the heat-treated cobalt macrocycles are stable over several hours in acid solution. The longer term stability of the polymer-based materials in acid has not been checked as yet. The stability of the heat-treated macrocycles has been found in our laboratory to be much less than that in alkaline solution. This is believed to be due to

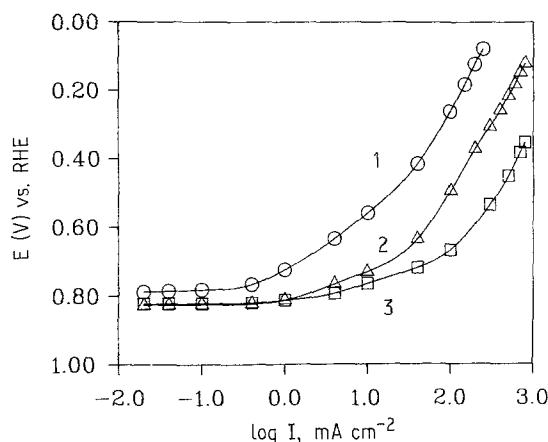


Fig. 12. Role of de-ashed RB carbon in the heat-treated PAN-based catalysts. Polarization curves with porous O_2 -fed (1 atm) electrodes in $85\% \text{ H}_3\text{PO}_4$ at 100°C . All the electrodes contained 20.8 mg cm^{-2} catalyst/carbon and 5.2 mg cm^{-2} Teflon. Curve 1, 40% PAN/DRB, 800°C HT. Curve 2, 40% PAN/DRB + 1.18% Co (added as the acetate), 800°C HT. Curve 3, 10% CoTMPP/DRB, 800°C HT.

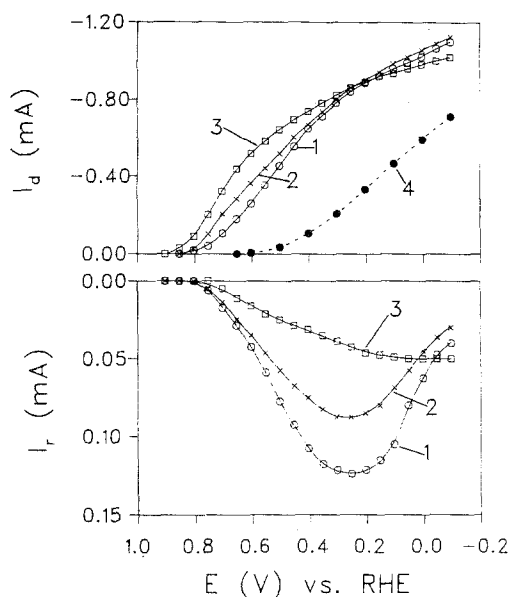


Fig. 13. Thin porous coating rotating ring-disk behavior for PAN-, PB- and macrocycle-based catalysts containing cobalt. Rotating ring-disk currents for O_2 reduction (1 atm) on thin porous coating (TPC) electrodes in 0.05 M H_2SO_4 at 25°C; disk area (geometric) = 0.196 cm^2 ; ring, Pt ($N = 0.37$), ring potential = +1.4 V; 2500 rpm; Teflon = ~10%. Curve 1, 5% CoTMPP/XC-72, 800°C HT. Curve 2, 40% PAN/XC-72 + 1.18% Co (added as the acetate), 800°C HT. Curve 3, PB + 2.5% Co (added as the acetate), 800°C HT. Curve 4, 40% PAN/XC-72, 800°C HT.

the greater solubility of Co ions in the acid electrolyte and their subsequent loss from the catalyst surface. These heat-treated catalysts retain their catalytic activity over longer periods in de-ashed RB carbon as the support probably because the small pores in the carbon impede the loss of the transition metal from the cathode. A promising approach for greatly slowing down the loss of the transition metal species from the cathode is to replace the fluid electrolyte within the pores with an ionically conducting polymer or to use such as a discrete polymer film blocking layer in contact with the solution side of the cathode [24].

The wetting properties of the two carbons (DRB and XC-72) may also cause differences in the performance. The fact that the overall performance of the heat-treated PAN/DRB is much better than that of the heat-treated PAN/XC-72 may also, in part, be due to a slight iron impurity (~0.31 wt%) present in the de-ashed RB carbon as compared to the XC-72 (~0.015 wt%). This also accounts for the smaller difference in the activities of the heat-treated Co/PAN/DRB and PAN/DRB (Fig. 12) as compared with the difference between Co/PAN/XC-72 and PAN/XC-72 (Fig. 11). The activity of Co/PAN/DRB (800°C HT) is similar to that of CoTMPP/DRB (800°C HT) at lower current densities ($< 1 \text{ mA cm}^{-2}$) but is lower at higher current densities. This may be due to the fact that the structure of porous gas-fed electrodes involving Co/PAN/DRB (800°C HT) has not been optimized.

Figure 13 gives the comparative ring and disk currents for O_2 reduction on PAN-, PB- and macrocycle-based catalysts containing cobalt and heat-treated at 800°C using the TPC electrode technique

in 0.05 M H_2SO_4 . At lower current densities, the apparent catalytic activity for O_2 reduction decreases in the following order: Co/PB > Co/PAN/XC-72 > CoTMPP/XC-72, while the ring currents increase in the same order. It may be noted that, even though the PB-based catalyst here exhibits better performance than does the PAN-based catalyst, the latter exhibits better performance in 85% H_3PO_4 at 100°C. None of the curves shows a well-defined diffusion-limiting current plateau, as in the case of 0.1 M NaOH mentioned earlier. This again appears to be an artifact of the porous coating electrode. The difference in activity of the PAN-based catalysts with and without cobalt is much greater in acid electrolyte than in alkaline electrolyte. This is due to the fact that carbon itself is a good catalyst for O_2 reduction to HO_2^- in alkaline electrolyte and a very poor catalyst in acid electrolyte. The ring currents for the PAN- and PB-based catalysts are practically negligible at lower polarizations ($> 0.7 \text{ V vs RHE}$) and may indicate a direct 4-electron reduction of O_2 to H_2O in addition to a 2-electron reduction process.

The structure of the PAN after heat treatment (800°C) in an inert atmosphere in the presence of cobalt salts is not known with any certainty. The structural investigation of heat-treated PAN of Teoh *et al.* [18] did not involve materials that had been heat-treated in the presence of transition metal salts. If the materials heat-treated with the transition metal salts contain the same fused pyrido-rings as the materials heat-treated without the transition metal, the nitrogen atoms of these rings could act as adsorption or coordination sites for the transition metal ions. These adsorbed metal ions could then act as catalytic sites for O_2 reduction to peroxide and for peroxide decomposition.

Figure 14 shows the diffuse reflectance spectra for the PAN samples with and without cobalt heat-treated at various temperatures. The spectra indicate the disappearance of the nitrile groups ($\sim 2250 \text{ cm}^{-1}$) after the heat treatment, with evidence for the production of pyrido-rings, as indicated by the $C=C$ ($\sim 1590 \text{ cm}^{-1}$) and $C=N$ ($\sim 1360 \text{ cm}^{-1}$) peaks. The presence of cobalt during the pyrolysis tends to stabilize the two broad peaks at $\sim 1590 \text{ cm}^{-1}$ and $\sim 1300 \text{ cm}^{-1}$ even at 800°C. This could be interpreted on the basis that a possible coordinative interaction of cobalt with the nitrogen of the pyrido-ring results in stabilizing a structure containing the $C=N$ and $C=C$ groups at 800°C. Elemental analysis shows that about 50% of the nitrogen is retained in such samples heat-treated at 800°C. The vibrational data, however, do not provide definitive evidence for the proposed binding of the Co to the pyridino-nitrogen due to the absence of far-infrared information corresponding to the cobalt-nitrogen vibration in the spectra. The Co may be coordinated to one or two adjacent pyridino-nitrogens and even to two or more nitrogens not adjacent to each other in separate sections of a particular polymer molecule or separate polymer molecules.

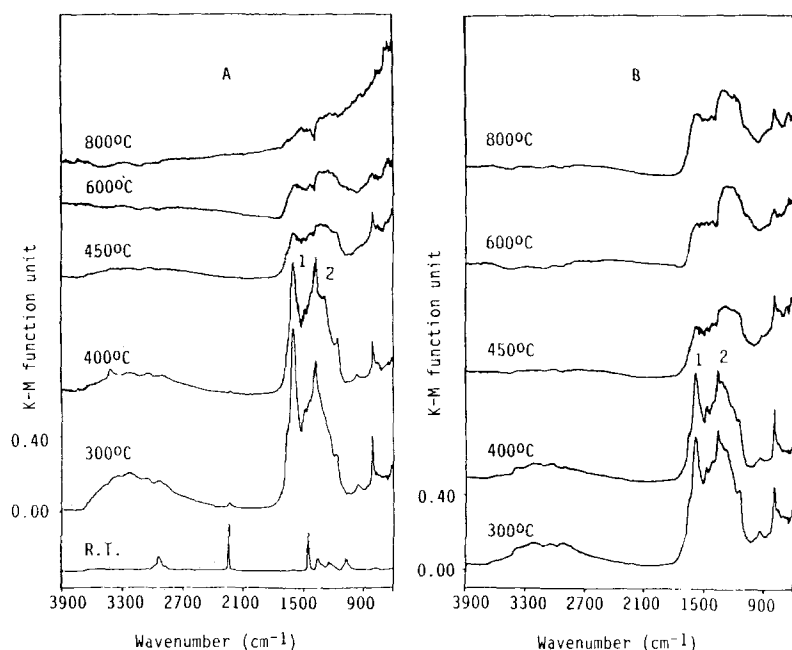


Fig. 14. Diffuse reflectance FTIR spectra of PAN samples heat-treated at various temperatures without (A) and with (B) Co (added as the acetate), 2% in KBr, 4 min grinding. The $K-M$ function = $(1 - R)^2/2R$, where R is the reflectance (see Ref. [27]).

Materials that may have some similarity with the ones mentioned here have been reported [25]. They are based on PAN together with Ir, Ru and Pt salts and have been developed for anode coatings in metal electro-winning cells in acid electrolytes. These are low-area materials and do not contain carbon black. These materials have not been examined spectroscopically, and thus it is not known whether they are structurally similar to the ones reported here.

4. Conclusions

The PAN-based catalysts, particularly Co/PAN/XC-72, show promising performance for O_2 reduction in alkaline and acid electrolytes. These catalyst systems function through a peroxide mechanism similar to that involved with the heat-treated cobalt porphyrins and have comparable apparent activity. Heat-treated preparations involving PAN with cobalt acetate and steam-activated Shawinigan acetylene black have shown good stability in the form of air cathodes when tested at the Electromedia Corporation (Englewood, NJ) under conditions appropriate for alkaline aluminum-air cells, better than that for heat-treated CoTMPP/SASB [26]. The lower cost of such polymer-based catalysts as compared with the CoTMPP macrocycle is also attractive. These studies further support the model proposed by the Case group to explain the catalytic activity of the heat-treated transition metal macrocycles for O_2 electroreduction.

Acknowledgement

This work was supported by the US Department of Energy through subcontracts with Lawrence Berkeley National Laboratory and Eltech Systems Corporation and the infrared studies by the U.S. Office of Naval Research.

References

- [1] H. Jahnke, M. Schoenborn and G. Zimmermann, *Topics in Current Chemistry* **61** (1976) 133.
- [2] V. S. Bagotzky, M. R. Tarasevich, K. A. Radyushkina, O. A. Levina and S. I. Andrusova, *J. Power Sources* **2** (1977/78) 233.
- [3] J. A. R. van Veen, J. F. van Baar and K. J. Kroese, *J. Chem. Soc., Faraday Trans. I* **77** (1981) 2827.
- [4] K. Wiesener and G. Gruenig, *J. Electroanal. Chem.* **180** (1984) 639.
- [5] I. Iliev, S. Gamburtsev, A. Kaisheva, A. Fuhrmann and K. Wiesener, *J. Power Sources* **13** (1984) 217.
- [6] D. Scherson, S. L. Gupta, C. Fierro, E. B. Yeager, M. E. Kordesch, J. Eldridge, R. W. Hoffman and J. Blue, *Electrochim. Acta* **28** (1983) 1205.
- [7] K. Okabayashi, O. Ikeda and H. Tamura, *Chem. Lett.* (1982) 1659.
- [8] D. Scherson, A. A. Tanaka, S. L. Gupta, D. Tryk, C. Fierro, R. Holze and E. B. Yeager, *Electrochim. Acta* **31** (1986) 1247.
- [9] K. A. Radyushkina and M. R. Tarasevich, *Elektrokhimiya* **22** (1986) 1155.
- [10] G. Gruenig, K. Wiesener, A. Kaisheva, S. Gamburtsev and I. Iliev, *Elektrokhimiya* **19** (1983) 1571.
- [11] S. L. Gupta, W. Aldred and E. B. Yeager, in 'Extended Abstracts', Vol. 83-2, The Electrochemical Society, Pennington, NJ (1983) p. 626.
- [12] R. Holze, D. Scherson, D. Tryk, S. L. Gupta and E. Yeager, in 'Extended Abstracts', 35th Meeting of the International Society of Electrochemistry, Berkeley, CA (1984) p. 399.
- [13] J. McBreen, W. E. O'Grady, D. E. Sayers and C. Y. Yang, in 'Extended Abstracts', Vol. 87-1, The Electrochemical Society, Pennington, NJ (1987) p. 746.
- [14] S. Gupta, D. Tryk, M. Daroux, W. Aldred and E. Yeager, in 'Proceedings of the Symposium on Load Levelling and Energy Conservation in Industrial Processes', (edited by D. Chin), The Electrochemical Society, Pennington, NJ (1986) p. 207.
- [15] S. Gupta, D. Tryk, W. Aldred, I. Bae and E. Yeager, in 'Extended Abstracts', Vol. 87-1, The Electrochemical Society, Pennington, NJ (1987) p. 455.
- [16] I. Bae, D. Tryk, S. Gupta and E. Yeager, manuscript in preparation.
- [17] E. Fitzer, K. Mueller and W. Schaefer, in 'Chemistry and Physics of Carbon' (edited by P. L. Walker Jr), Marcel Dekker, New York (1971) Vol. 7, pp. 237-383.
- [18] H. Teoh, P. D. Metz and W. G. Wilhelm, *Mol. Cryst. Liq. Cryst.* **83** (1982) 297 and references therein.

- [19] S. Clouser, Ph.D. Dissertation, Case Western Reserve University (1981) p. 58.
- [20] I. Bae, Case Western Reserve University, unpublished results.
- [21] E. Delmonde and M. Pourbaix, in 'Atlas of Electrochemical Equilibria in Aqueous Solutions' (edited by M. Pourbaix), Pergamon, Oxford (1966) pp. 322-329.
- [22] Yu. V. Pleskov and V. Yu. Filinovskii, 'The Rotating Disc Electrode', Consultants Bureau, New York (1976) pp. 90-92.
- [23] R. E. Carbonio, D. Tryk and E. Yeager, in 'Proceedings of the Symposium on Electrode Materials and Processes for Energy Conversion and Storage' (edited by S. Srinivasan, H. Wroblowa and S. Wagner), The Electrochemical Society, Pennington, NJ (1987) pp. 238-255.
- [24] M. S. Hossain, D. Tryk and E. Yeager, in 'Extended Abstracts', Vol. 87-1, The Electrochemical Society, Pennington, NJ (1987) p. 466.
- [25] H. Hinden and J. Gauger, *J. Electrochem. Soc.* **133** (1986) 692.
- [26] F. Solomon, private communication, May 1987.
- [27] M. P. Fuller and P. R. Griffiths, *Anal. Chem.* **50** (1978) 1906.